

UC Davis

UC Davis Previously Published Works

Title

Strategies for the Immobilization and Signal Amplification of a Double Nanobody Sandwich ELISA for Human Microsomal Epoxide Hydrolase.

Permalink

<https://escholarship.org/uc/item/0q54t2mt>

Journal

Analytical Chemistry, 96(49)

Authors

He, Qiyi

Pan, Bofeng

McCoy, Mark

et al.

Publication Date

2024-12-10

DOI

10.1021/acs.analchem.4c04505

Peer reviewed

Strategies for the Immobilization and Signal Amplification of a Double Nanobody Sandwich ELISA for Human Microsomal Epoxide Hydrolase

Qiyi He, Bofeng Pan, Mark McCoy, Junkang Pan, Zhihao Xu, Christophe Morisseau, Gang Sun, Dongyang Li,* and Bruce D. Hammock*



Cite This: *Anal. Chem.* 2024, 96, 19605–19614



Read Online

ACCESS |



Metrics & More

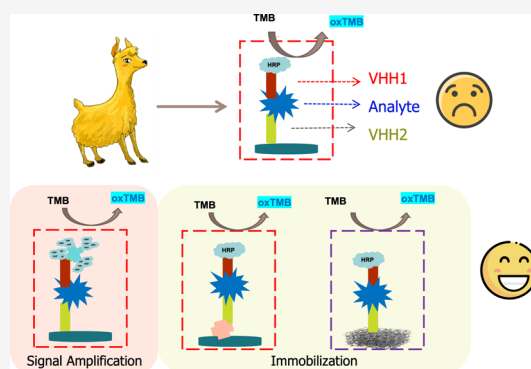


Article Recommendations



Supporting Information

ABSTRACT: The microsomal epoxide hydrolase (mEH) is important in the detoxification of carcinogens in the liver and other tissues but is also a blood biomarker of hepatitis and liver cancer. Improved analytical methods are needed for the study of its role in the metabolism of xenobiotics and endogenous roles as a blood biomarker of diseases. The development of a double nanobody sandwich ELISA offers significant improvements over traditional polyclonal or monoclonal antibody-based assays, enhancing both the homogeneity and the stability of assay production. This study focuses on selecting and optimizing nanobody pairs for detecting human mEH. Four high-affinity nanobodies were identified and tested for thermal stability. Combinations of these nanobodies were evaluated, revealing that the MQ4–MQ30 pair achieved the best performance with a limit of detection (LOD) of 1 ng/mL. Additionally, polyHRP was also employed for signal amplification, enhancing detection capabilities despite challenges related to the small size and single epitope recognition of the nanobodies. Comparative studies using microplates and NHS@MF membranes were also performed. The superior performance of the NHS@MF membranes highlighted their potential as a promising alternative for point-of-care testing. The assay exhibited high specificity for human mEH and minimal cross-reactivity with related enzymes and effectively addressed matrix effects in plasma and tissue samples. These findings underscore the potential of double nanobody sandwich ELISAs for reliable and sensitive biomarker detection.



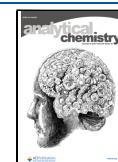
INTRODUCTION

Epoxide hydrolases are α/β hydrolase fold enzymes that hydrolyze cyclic ethers known as epoxides to the corresponding diols. The microsomal epoxide hydrolase (mEH, *EPHX1*, EC 3.3.2.9) was the first discovered mammalian epoxide hydrolase. It was initially studied for its role in the conversion of carcinogenic epoxides of polycyclic aromatic hydrocarbons, pesticides, and other xenobiotics to vicinal diols.^{1–3} Such diols are not alkylating agents and are more easily excreted. More recently, it has also been suggested that mEH is involved in regulating natural epoxy-fatty acids (EpFAs) that in turn resolve inflammation and regulate other biological functions in the organism, and their imbalance can lead to diseases.^{4,5} Additionally, the expression of high activity mEH mutants has been associated with the development of several diseases, including cancer, preeclampsia, and neurological disorders.^{6–9} The presence of mEH in plasma has been strongly correlated with Kaposi's sarcoma metastasis to the liver.¹⁰ Furthermore, mEH has been detected in the plasma of patients with hepatitis C and A virus infections.¹¹ The mEH levels in tissues and body fluids may provide valuable information for epidemiological studies, pharmacological treatments, and disease diagnostics.

Therefore, the development of mEH detection could serve as an important diagnostic tool for human health, offering insights into biological metabolism.

Among the methods used to selectively detect a protein, immunological assays based on the specific binding between antibody and antigen are the most promising for rapid, high-throughput, and quantitative detection of biomolecules in patient tissues and biofluids. New-generation engineered antibodies, represented by the variable domain of heavy chain (VHH), have attracted extensive attention due to their unique advantages.^{12,13} Also known as nanobodies, VHHs consist of a single antigen-binding domain with a molecular weight of approximately 15 kDa. Benefiting from phage display technology, researchers can easily retrieve and use these

Received: August 22, 2024
Revised: November 11, 2024
Accepted: November 12, 2024
Published: November 22, 2024



nanobodies. Since then, many nanobodies have been developed and applied in various fields such as medical diagnosis, therapy, environmental pollutants, and monitoring of foodborne microbes.^{14,15}

Nanobodies are widely used in the immunological analysis of small molecules employing competitive immunoassay methods, which often require only a single nanobody to construct the assay.¹⁶ However, for the detection of macromolecules, double-antibody-based sandwich immunoassays are typically used. In these assays, nanobodies mostly serve as detection antibodies, while traditional polyclonal or monoclonal antibodies are used as capture antibodies.^{17,18} The limited use of double-nanobody-based sandwich immunoassays can be attributed to several reasons: (1) the difficulty in selecting paired nanobodies from a limited pool of positive clones; (2) the small size makes them challenging to immobilize on polystyrene plastic plates through physical adsorption, and nonspecific binding may occur; and (3) the insufficient amplitude in signal output resulting from the lack of amplification from a secondary antibody. The limitations of paired nanobodies can be addressed through affinity maturation prior to screening for nanobodies, increasing the capacity of phage libraries, or optimizing screening strategies.¹⁹ Given the premise of obtaining paired nanobodies through biopanning, the sensitivity of double nanobody sandwich immunoassays can be improved through two key approaches: immobilization and signal amplification. Several approaches have been employed to enhance the immobilization efficiency of the nanobodies. A convenient method has been to use streptavidin as a bridge to immobilize capture antibodies on microplates, which can significantly improve the sensitivity of double nanobody sandwich ELISA.^{20,21} There were also several effective strategies for maximizing nanobody exposure, including developing fenobodies and bispecific nanobodies.^{22–24} From the perspective of the signal output, there was also research on using phage-encoding nanobodies displayed as detection antibodies to amplify the output signal to compensate for insufficient antibody immobilization.²⁵ Signals can also be improved with alternative detection systems. For example, polyHRP is an ideal reagent that forms a supra-molecular polymer of horseradish peroxidase (HRP), capable of incorporating up to 400 enzyme molecules.¹³ It can bind to various ligands and receptors (e.g., streptavidin) and has been shown to improve sensitivity by up to 100-fold.¹³ Moreover, it is a commercially available reagent that is suitable for a wider range of research groups.

As a model for testing improved analytical methods for detecting proteins, we utilized double nanobody sandwich immunoassays to detect human mEH. In a previous work, we successfully expressed and purified the recombinant human mEH, and we constructed a phage display library using an immunized llama. Four unique encoding nanobodies were selected from the library for the detection of human mEH. A sandwich immunoassay method using a monoclonal antibody as a capture antibody and a nanobody as a detection antibody was developed, while polyHRP was also used as a signal amplification label, improving the sensitivity of the reaction.²⁶ However, this sandwich immunoassay relied on the production of stable and consistent batches of monoclonal antibodies, whereas genetically encoded nanobodies can yield consistent proteins with extremely high purity, reducing risks of variations between batches. In this study, we investigated different strategies for the development of double nanobody sandwich

immunoassays as depicted in Figure 1. One approach involved using streptavidin as a bridge to immobilize nanobodies on

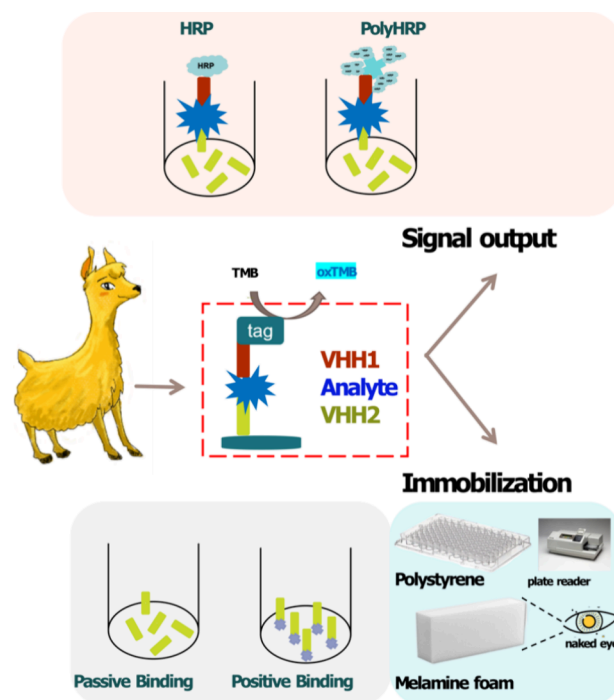


Figure 1. Diagram of the development of double nanobody sandwich immunoassays for human mEH.

microplates to optimize nanobody noncovalent fixation to the microplate. The second approach, to increase the assay sensitivity, utilized SA-polyHRP as an enzyme-linked signal reagent. Additionally, NHS-modified melamine-formaldehyde foam (MF) was used as an assay support, with nanobodies covalently attached to it. MF is a network polymer with a unique macroporous, three-dimensional, homogeneous, and reticulated framework, featuring pores of 100–200 μm and an average framework diameter of $\sim 7 \mu\text{m}$.²⁷ In general, these structural features make MF advantageous because of its low density, high compressibility, excellent sound absorption, low fluid resistance, and effective surface contact, leading to the widespread use in cleaning, insulation, acoustic absorption, filtration, and purification. When applied as a matrix for immunoassays, these unique features offer several advantages including enhanced immobilization efficiency, excellent mechanical properties, and increased surface area for binding. Additionally, the matrix allows the free movement of biomolecules of various sizes in all directions within the framework, leading to improved efficiency and effectiveness in target molecule detection.²⁸ This interconnected structure promotes chaotic and vortex mixing, thereby increasing the frequency of contacts between biomolecules and the framework's surfaces. Building on these advantages, we explored the use of MF in a novel application as a matrix for a double-nanobody-based immunoassay. Specifically, a paper-based double nanobody sandwich immunoassay was developed, designed to facilitate naked-eye observation for practical and accessible diagnostics. In this section, we compared the sensitivity of two different immobilization carriers: traditional microplates and melamine foam. The comparison aimed to assess whether the unique structural and chemical properties of

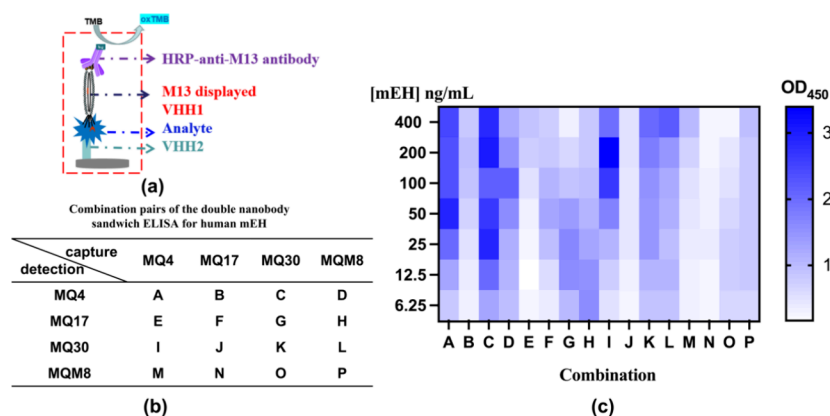


Figure 2. (a) Schematic diagram of the proposed sandwich nanobody immunoassay. (b) Combination pairs of the double nanobody sandwich ELISA for human mEH. (c) Heat map result of the different combinations of nanobody pairs by applying a series concentration of human mEH in sandwich ELISA. One hundred microliters of 1 $\mu\text{g/mL}$ MQ4 was incubated to a microplate, and then a series concentration of human mEH was added. A 10^{10} pfu/mL phage displaying corresponding VHH was then applied as the detection antibody followed by adding the HRP labeled anti-M13 antibody. Subsequently, the TMB solution was used for signal development. Error bars indicate standard deviations ($n = 3$).

MF could outperform conventional microplates in enhancing the assay sensitivity and overall performance. These simple and sensitive double-nanobody-based ELISAs were applied to determine the mEH content in practical samples and validated by using a radiometric assay for enzyme activity testing.

EXPERIMENTAL SECTION

Materials. Antihuman mEH VHHs and human mEH recombinant protein were prepared as described in our previous work.²⁶ Streptavidin-HRP conjugate (SA-HRP) was purchased from Southern Biotech (Birmingham, AL). The anti-HA tag antibody with HRP was purchased from Roche (NJ, USA). Streptavidin polyHRP40 conjugate (SA-polyHRP) was purchased from Fitzgerald Industries International (Concord, MA). Streptavidin, plasma from human, sodium periodate, sulfo-NHS-LC-biotin, and 3,3',5,5'-tetramethylbenzidine (TMB) were obtained from Sigma-Aldrich (St. Louis, MO). Unless otherwise specified, all other chemicals and reagents used were analytical grade.

Selection of Nanobody Pairs. First, we screened approximately 96 phage display clones for binding to the mEH. Secondary screens were selected based on high affinity for the mEH, and then we evaluated paired combinations of four nanobodies specifically recognizing mEH to establish an immunoassay method by utilizing a double nanobody sandwich ELISA. Specifically, there were 16 pairings in total among the four nanobodies (including homologous pairings). Briefly, 100 μL /well of different VHHs (1 $\mu\text{g/mL}$) was added and immobilized to the microplate at 4 $^{\circ}\text{C}$ overnight, washed with PBST, and blocked with 3% skim milk. Subsequently, the mEH recombinant protein standards (ranging from 0 to 400 ng/mL) were added, and the mixture was incubated at room temperature for 1 h. After washing with PBST, the corresponding phage display nanobodies (10^{10} pfu/mL) were added to each well. Following 1 h of incubation at room temperature, HRP labeled anti-M13 antibody was added. After 1 h of incubation and washing with PBST, TMB substrate solution was added for color development. The reaction was terminated by adding sulfuric acid, and the absorbance at 450 nm was read on an M2 microplate reader (Molecular Devices, San Jose, CA).

Double Nanobody Sandwich-Based ELISA on the Microplate. Based on the screened paired nanobodies, we constructed methods for double nanobody sandwich-based ELISA on a microplate using the streptavidin–biotin system to establish methods from the perspective of optimizing coating and signal amplification, respectively. Considering the immobilization aspect, for example, streptavidin was coated on the microplate followed by blocking with 2% BSA in PBS, and then the biotinylated MQ4 was added. After washing with PBST, a series of concentrations of authentic human mEH (or samples) were added and incubated for 1 h at room temperature followed by incubation with HRP-labeled MQ30 for another 1 h before color development. From the signal improvement perspective, MQ4 was directly immobilized on the microplate followed by blocking with 3% skim milk in PBS. After PBST washing, a series of concentrations of recombinant human mEH were added and incubated for 1 h followed by the biotinylated MQ30. After another round of PBST washing, SA-polyHRP was added for the signal output. In both cases, color development was achieved through HRP catalyzing TMB substrate, and the reaction was terminated using sulfuric acid, followed by reading OD₄₅₀ results for analysis.

Double Nanobody Sandwich-Based ELISA on the Melamine Foam Membranes. Melamine foam membranes in 1 mm thick slices and 5 mm diameter were manufactured and chemically modified by NHS as previously described.²⁷ Briefly, 100 μL of the nanobody (MQ4, 1 $\mu\text{g/mL}$) was added to the NHS@MF membranes and incubated for 1 h at room temperature. After washing with PBST, 100 μL of 3% skim milk was added to block the unspecific binding. After 1 h, the membranes were washed with PBST, and then 100 μL of varying concentrations of human mEH (ranging from 0 to 1000 ng/mL) and samples was added to each membrane and incubated for 1 h. After washing with PBST, 100 μL of nanobody labeled HRP (MQ30-HRP, 1 $\mu\text{g/mL}$) was added. After 1 h, the membranes were washed five times with PBST and dried in the air. Then, 25 μL of the TMB substrate was added to the membranes, and the membranes were placed in an LED light box. A smartphone (iPhone XR) captured the colorimetric signal generated by the interaction between HRP and the TMB substrate. The data for RBD analysis were subsequently processed using the Photoshop (Adobe) software.

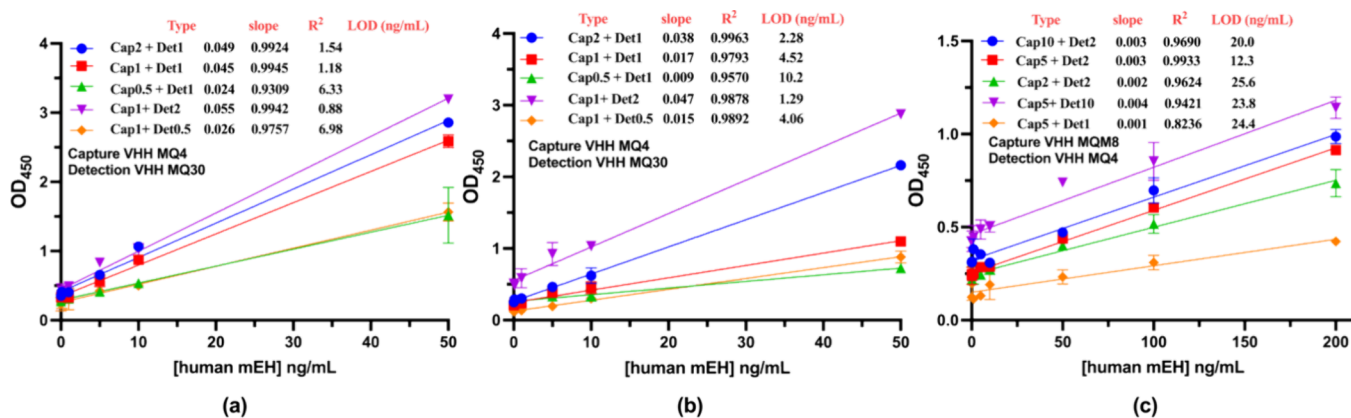


Figure 3. Optimization of the concentration of capture antibody and detection antibody with different nanobody pairs by sandwich ELISA. Streptavidin was preimmobilized on the plate, the biotinylated nanobody was applied as the capture antibody, and the HRP labeled antibody was used as the detection antibody. (a) Dual nanobody sandwich ELISA using VHH MQ4 as the capture antibody and VHH MQ30 as the detection antibody. (b) VHH MQ30 as the capture antibody and VHH MQ4 as the detection antibody. (c) VHH MQM8 as the capture antibody and VHH MQ4 as the detection antibody. Cap1 + Det1 stands for capture antibody concentration (1 $\mu\text{g}/\text{mL}$) + detection antibody concentration (1 $\mu\text{g}/\text{mL}$). Error bars denote the standard deviation ($n = 3$).

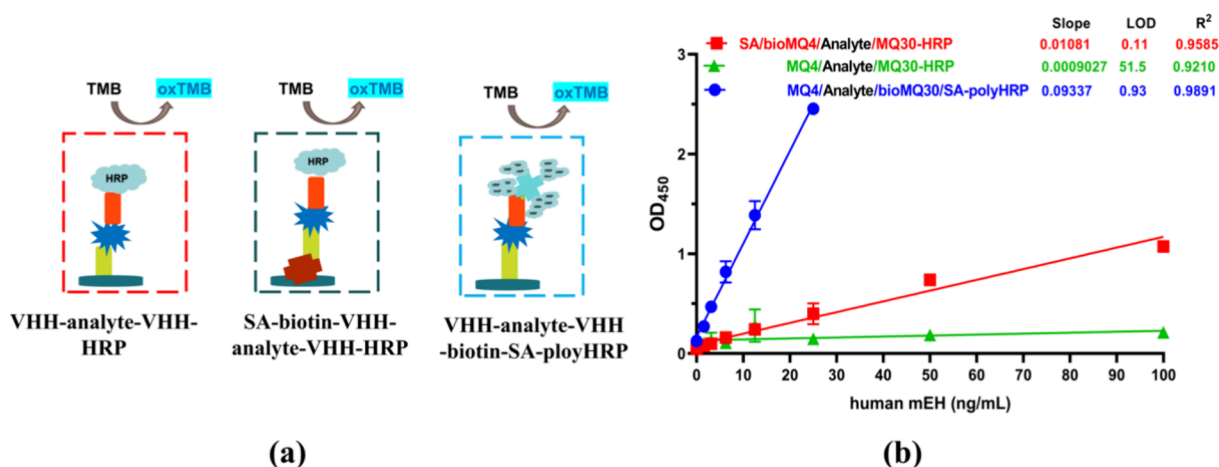


Figure 4. (a) Schematic diagram of three kinds of sandwich nanobody immunoassays. (b) Comparison of different formats of sandwich ELISA for the detection of human mEH. MQ4 (1 $\mu\text{g}/\text{mL}$) or biotinylated MQ4 was added as the capture antibody, while MQ30 or biotinylated MQ30 was applied as the detection antibody. Error bars denote the standard deviation ($n = 3$).

Cross-Reactivity. To evaluate the selectivity of the proposed double nanobody sandwich ELISA for mEH, we conducted tests to detect various epoxide hydrolases including mEH from different species (rat mEH) and other human epoxide hydrolases (human sEH, EH3, and EH4), which were spiked into PBS at a final concentration of 1000 ng/mL. The prepared enzyme samples were then analyzed by using double nanobody sandwich-based ELISA on microplate and NHS@MF membranes, alongside standard solutions of recombinant human mEH.

Sample Analysis and Method Validation. Whole tissue extracts from six different human commercial tissue samples (BioChain Institute, CA, USA) were obtained. These extracts were subjected to testing using proposed immunoassays at dilutions of 10^3 , 10^4 , and 10^5 -fold on microplates and at 20- and 50-fold dilutions on NHS@MF membranes. The accuracy of the results was confirmed by monitoring enzyme catalytic activity, as previously reported using [^3H]-*cis*-stilbene oxide as the substrate.²⁹

RESULT AND DISCUSSION

Selection of Nanobody Pairs for Double Nanobody Sandwich ELISAs. In traditional sandwich ELISA, capture antibodies are immobilized on microplates to catch the analytes, which are then quantified by enzyme-labeled detection antibodies. Benefiting from the unique advantages of nanobodies, developing a sandwich ELISA based on double nanobodies can entirely replace the use of polyclonal antibodies (pAb) or monoclonal antibodies (mAb), thereby enhancing the homogeneity of assay production and the stability of assay kits. In concept, the nanobodies are “immortal” because they can be easily regenerated from the DNA sequence should store aliquots be lost. Previously, four unique nanobodies had been identified with high affinity to human mEH²⁶. The thermal stability tests of four nanobodies were conducted by incubating the nanobodies and monoclonal antibodies at different temperatures for 30 min followed by direct ELISA to evaluate the remaining activity of the antibodies. As shown in Figure S1, the monoclonal antibodies completely lost their functionality after treatment at 80 °C, whereas the nanobodies maintained at least 60% of their

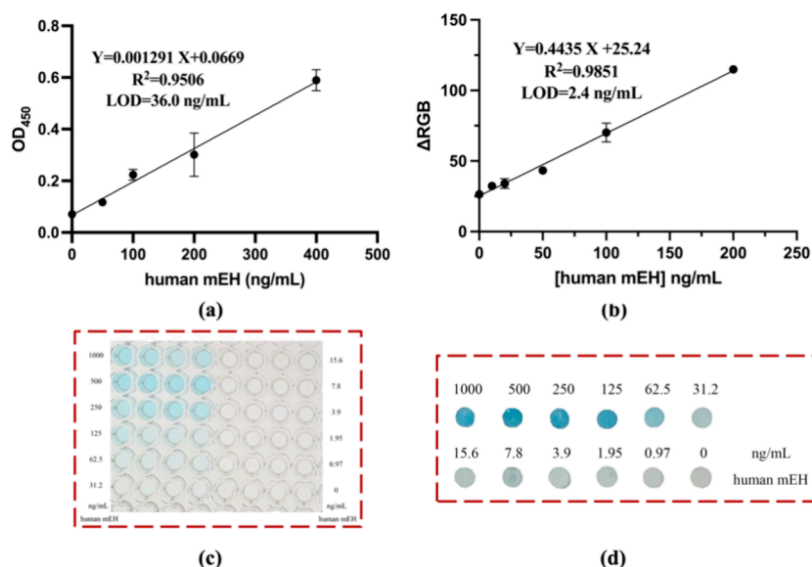


Figure 5. Calibration curves and the corresponding optical image of the double nanobody sandwich ELISA by microplate (a, c) and NHS@MF membranes (b, d). One hundred microliters of 1 $\mu\text{g}/\text{mL}$ MQ4 was incubated to the microplate and NHS@MF membranes, and then a series concentration of human mEH was added. MQ30-HRP (2 $\mu\text{g}/\text{mL}$) was then applied as the detection antibody followed by a TMB solution for signal development. Error bars indicate standard deviations ($n = 4$ for microplate and $n = 3$ for NHS@MF).

activity. Particularly, MQ4 and MQM8 retained over 50% activity even at the extreme temperature of 95 $^{\circ}\text{C}$. The data showed that the thermal stability of different nanobodies is not all identical but that they are more stable than the monoclonal antibody used for comparison.

To find suitable paired nanobodies, combinations of the four nanobodies, as depicted in Figure 2, were tested. Combination A, C, and I exhibited a notable concentration-dependent increase, whereas combination L also showed a positive trend, indicating that those combination formats were suitable for the establishment of double nanobody sandwich ELISA for human mEH. The homologous nanobodies (combination A) were also capable of forming a self-pair sandwich ELISA, possibly due to the mEH forming a polymer when released from membrane, with the nanobody pair recognizing repeated epitopes. The study was further focused exclusively on the heterologous nanobody pairs that are more sensitive. Subsequently, optimization experiments were conducted on the nanobody amounts for the three combinations to determine the optimal heterologous nanobody pair. As shown in Figure 3, the MQ4–MQ30 combination format demonstrated the best sandwich performance, achieving a limit of detection (LOD) of around 1 ng/mL. The LOD was calculated as $3S_B/k$, where S_B represented the standard deviation of the blank and k is the slope from the linear regression equation $y = kx + i$, with i as the intercept. In contrast, the MQM8–MQ30 format was less efficient with an approximately 20-fold higher LOD. Here, the MQ4–MQ30 combination was selected for subsequent experiments.

Comparison of Different Formats of Sandwich ELISAs on the Microplate. Different from the conventional double sandwich ELISA utilizing the polyclonal or monoclonal antibody, nanobodies face several challenges when being coated onto polystyrene microplates, primarily due to their small size. These issues lead to difficulties in physical adsorption and suboptimal orientation of the immobilized nanobody; the recognition site could be facing the solid matrix and be unavailable to catch the analyte. Additionally, given the

limited amount of immobilized nanobodies and lack of amplification of the reporting signal, the signal output from conventional ELISA reagents is insufficient to sensitively detect the analyte, which could limit the use of double nanobody sandwich ELISA applications. Therefore, taking advantage of the high affinity and specificity of the avidin–biotin interaction, two pathways to increase the applicability of double nanobody ELISA were investigated. The first approach involved coating the plate with streptavidin followed by the addition of biotinylated nanobodies to increase the amount of optimally oriented capture nanobody. The second approach involves the use of polyHRP to amplify the reporting signal.

For the first approach, after the introduction of the analyte, the HRP-labeled MQ30 reporting nanobody was used. Upon optimizing the concentrations of streptavidin and biotinylated nanobodies (Figure S2a), 2.5 $\mu\text{g}/\text{mL}$ streptavidin and 1 $\mu\text{g}/\text{mL}$ biotinylated MQ4 were selected for further optimization. Additionally, as shown in Figure S2b, using PBS containing skim milk as the buffer when adding HRP-labeled nanobodies can further reduce the nonspecific binding, which is crucial for enhancing the sensitivity of the assay. The adjusted slope of the regression reflects the assay sensitivity, emphasizing the correlation between the optical density and increasing analyte concentrations. As shown in Figure 4, the assay developed with streptavidin immobilization reached a sensitivity of 0.01081 OD mL/ng and LOD of 0.11 ng/mL with 468-fold lower LOD and a 12-fold higher sensitivity than the format merely applied with nanobodies.

HRP is an enzyme commonly used in ELISA, generating a detectable signal such as luminescence or color reaction, thus acting as an important tool in ELISA quantitation. PolyHRP is an ideal and evolutionary substitute for HRP. PolyHRP is a supermolecular polymer incorporating up to 400 molecules of HRP. Because the efficiency of immobilization of nanobodies on polystyrene microplate appeared limited and insufficient, signal output amplification is crucial for the development of a sensitive method. The introduction of polyHRP not only enhanced the color reaction of positive samples but also

Table 1. Spike-and-Recovery Analysis of Human mEH in Spiked Plasma Samples by Different Immunoassays on the Microplate

spiked (ng/mL)	SA/bioVHH/analyte/VHH-HRP				VHH/analyte/bioVHH/SA-ployHRP							
	1:10 dilution		1:100 dilution		1:10 dilution		1:100 dilution		1:1000 dilution			
	founded ^a (ng/mL)	recovery (%)	founded (ng/mL)	recovery (%)	founded (ng/mL)	recovery (%)	founded (ng/mL)	recovery (%)	founded (ng/mL)	recovery (%)		
50	33.6 ± 2.8	67	40.7 ± 1.9	81	58.7 ± 2.1	117	6.14 ± 0.17	77	7.86 ± 0.82	98	6.53 ± 0.63	82
25	20.4 ± 0.3	81	26.9 ± 0.5	108	27.5 ± 0.4	110	4.65 ± 0.12	116	4.66 ± 0.15	117	4.50 ± 0.12	112
12.5	10.9 ± 1.7	87	14.9 ± 0.4	119	13.3 ± 0.3	106	2.08 ± 0.08	104	2.20 ± 0.13	110	2.12 ± 0.18	106
6.25	5.8 ± 0.9	93	6.8 ± 0.1	109	6.5 ± 0.7	105	0.87 ± 0.06	87	1.15 ± 0.01	115	1.20 ± 0.07	120

^aResults are average ± SD (CV, *n* = 3).

increased the nonspecific binding of negative samples. To further reduce nonspecific binding, a different blocking strategy for the polyHRP system was optimized. Because of the involvement of the biotin–streptavidin system, the blocking effects of skim milk powder and BSA with PBS as the blocking buffer were investigated. In addition to the conventional blocking step performed after coating the capture nanobody, the blocking buffer was also applied when adding the detection nanobody to further reduce nonspecific binding. As shown in Figure S3, using BSA in PBS as the blocking buffer resulted in the highest nonspecific binding, while the absorbance at 450 nm of the blank samples was around 0.8, resulting in a narrow detection range. It was also observed that skim milk powder was superior to BSA in terms of blocking effectiveness and had minimal impact on the biotin–streptavidin system despite containing a small amount of biotin. Therefore, skim milk powder was selected as the preferred blocking reagent in the following experiments. After the optimization, the performance of VHH/analyte/bioVHH/SA-ployHRP, along with the other two approaches, is shown in Figure 4. The assay utilizing polyHRP for signal amplification achieved a sensitivity of 0.09337 OD·mL/ng and an LOD of 0.93 ng/mL, showing a 55-fold lower LOD and a 103-fold higher sensitivity compared to the format that used only nanobodies and the standard HRP reporter system. Notably, the VHH/analyte/bioVHH/SA-ployHRP format exhibited nearly 10 times higher LOD and sensitivity compared to SA/bioVHH/analyte/VHH-HRP.

NHS@MF vs Microplate. Under optimal conditions (depicted in Figures S4–S6), the establishment of double nanobody sandwich ELISA by NHS@MF membranes was compared with the ELISA by a microplate. Except for the different “medium” used, all other experimental conditions, including reagent concentrations, reaction time, etc., were the same. As depicted in Figure 5a,c, the ELISA with the microplate showed a sensitivity of 0.0013 OD·mL/ng and an LOD of 36.0 ng/mL. In Figure 5b,d, the assay applied to NHS@MF membranes was developed and reached an LOD of 2.4 ng/mL, which is 15-fold lower than the microplate format. Compared to “traditional” microplates, the image demonstrated that using NHS@MF membranes for chemical conjugation to immobilize nanobodies can significantly enhance the coating efficiency. Moreover, the unique 3D macroporous reticulated structure of NHS@MF allows for the rapid mass transfer of large biomolecules through the framework in all directions. This structural feature ensures excellent accessibility of the entire active binding sites on the framework to the target molecules, resulting in significantly increased intensity of colorimetric signals, making it easier to visually observe color variations, which positions it as a promising material for point-of-care testing (POCT).³⁰ Notably, our previous study revealed that using nanobodies as capture antibodies in melamine foam-based biosensors significantly improved their storage stability compared to that of using full-length antibodies. Without the existence of any stabilizers, the colorimetric signal of the nanobody-based sensors retained over 70% of its original intensity after 30 days of storage at room temperature.³⁰ By using double nanobodies, the proposed ELISAs demonstrated high stability, attributed to the unique structural properties of nanobodies, which offer enhanced resistance to extreme pH and temperature.^{31,32}

Cross-Reactivity. The selectivity of the double nanobody immunoassay was assessed using ELISA assays on NHS@MF membranes and microplates. Spiked with 1000 ng/mL

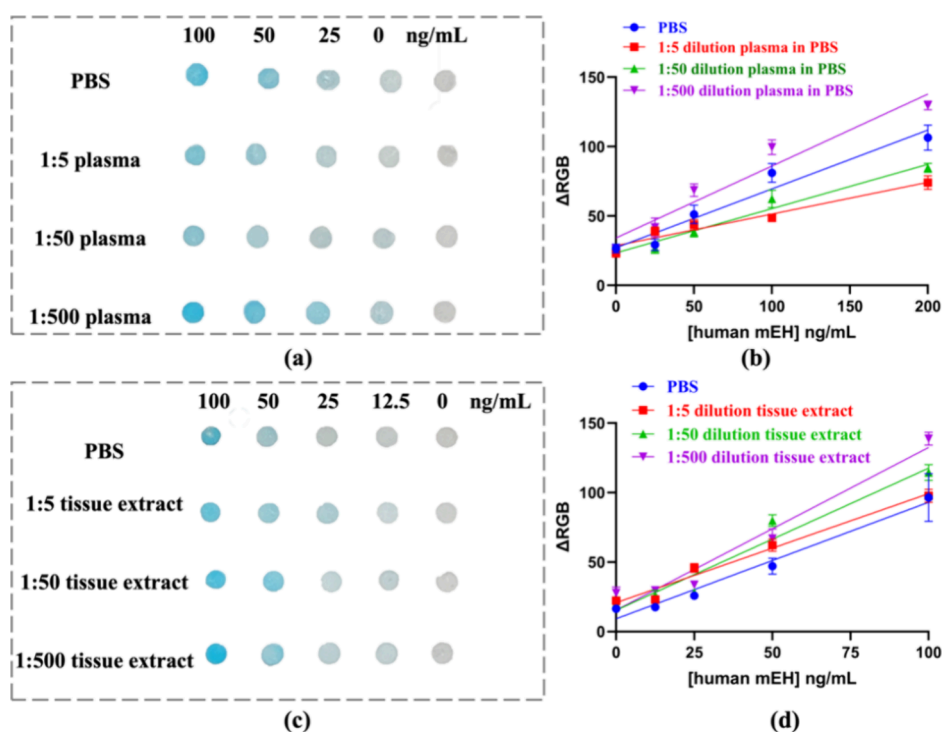


Figure 6. Spike-and-recovery assay of the double nanobody sandwich ELISA for human mEH on NHS@MF membranes. The optical images (a, c) and plots (b, d) for the spike-and-recovery test for the NHS@MF membranes-based immunoassay in human plasma and mice brain tissue extract. Error bars indicate standard deviations ($n = 3$).







recombinant human mEH, rat mEH, and other human epoxide hydrolases (EH3 and EH4), samples were analyzed using the NHS@MF membranes, while a series concentration of those same epoxide hydrolases was added to the microplate for absorbance measurement. Figure S7a reveals that only the mEH could be visually identified among samples spiked with 1000 ng/mL of epoxide hydrolases, whereas other target enzymes did not result in chromogenic reactions. Cross-reactivities (CR) were determined using the following formula: $CR (\%) = [\text{measured concentration of the analogs/spiked concentration of the analogs}] \times 100\%$. The assay demonstrated minimal cross-reactivity with denatured mEH (0.18%) and rat mEH (1.56%) showing slight reactivity. No cross-reactivity was observed with human sEH, human EH-3, and human EH-4. A similar result was obtained in the microplate and is shown in Figure S7b. Therefore, the method exhibited a high level of specificity because did not recognize denatured proteins, and notably, it did not exhibit cross-reactivity with rat sEH despite an 80% similarity in gene sequences, and even lower similarity was noted for human sEH, human EH-3, and human EH-4. These findings illustrated the strong selectivity of the proposed double nanobody sandwich ELISA method for human mEH because it takes advantage of the high specificity of the two individual nanobodies and requires that both nanobodies bind to the target analyte for a signal to appear.

Matrix Effects. To assess the potential interference or impact within a sample matrix and ensure the accuracy and reliability of analytical results, the matrix effect was investigated by applying it in the plasma and tissue extracts. Dilution of samples is commonly employed to mitigate matrix effects, although then, greater demands are placed on assay sensitivity. Herein, the spike-and-recovery analysis in spiked plasma samples was conducted by different immunoassays on microplates with 1:10, 1:100, and 1:1000 dilution of the

human plasma spiked with human mEH (see Table 1). The recoveries were 67–116, 81–119, and 82–120% for 1:10, 1:100, and 1:1000, respectively. It can be observed that there was a matrix effect at a dilution ratio of 1:10. However, increasing the dilution ratio effectively reduces the matrix effect in plasma. In tissue extracts, those proposed methods also demonstrated good reproducibility (Table S1). Intra-assay and interassay variabilities were evaluated, with coefficients of variation (CVs) ranging from 0.2 to 18.8% across 1:10 to 1:1000 dilutions of mice brain tissue extract samples, indicating robust reproducibility across different dilution ratios of tissue extracts. Therefore, the development of highly sensitive analytical methods to adapt to higher dilutions for reducing matrix effects is crucial for the practical application of the method. The matrix effect of the double-nanobody-based immunoassay on NHS@MF membranes was also investigated. As shown in Figure 6a,b, the NHS@MF membrane-based ELISA exhibited matrix effects in human plasma, and dilution partially alleviated them. When the plasma was diluted 500-fold, accurate and reliable analytical results could be obtained. The matrix effect of the tissue extract was also investigated because the subsequent test for mEH detection was applied within the tissue extract. From Figure 6c,d, it can be observed that there was a matrix effect in the tissue, but this effect was mitigated when there was a fivefold dilution of the sample.

Biological Sample Analysis. Double nanobody sandwich ELISAs were applied to detect human mEH in human tissue samples. Three kinds of ELISAs with microplates and NHS@MF membranes and enzyme activity were used to analyze the same samples. As shown in Table 2, the results of the ELISAs were comparable to the enzyme activity based on the radiometric assay by using $^3\text{H } c\text{-SO}$ as the substrate. Despite the significant differences between the data obtained through the RGB analysis from NHS@MF and the absorbance values

Table 2. A Comparison of Double Nanobody Sandwich ELISA and Enzyme Activity Test for the Analysis of Human MEH in the Human Tissue Whole Cell Extract Samples

Human tissues	Enzyme activity ^b	mEH concentration (nM) ^a			VHH/analyte/VHH-HRP (NHS@MF membrane)	Optical image
		SA/bioVHH/analyte/VHH-HRP	VHH/analyte/bioVHH/SA-ployHRP			
liver	850±50	170.63±12.54	135.46±8.11	152.42±16.19		
					50 × dilution	
kidney	22±11	N.D.	N.D.	8.14±2.66		
					20 × dilution	
lung	20±2	4.43±0.40	1.73±0.13	33.29±4.48		
					20 × dilution	
adrenal	290±50	10.69±1.50	8.09±0.64	43.55±5.22		
					20 × dilution	
heart	10±4	N.D.	N.D.	N.D.		
					20 × dilution	
spleen	6±1	N.D.	N.D.	N.D.		
					20 × dilution	

^aResults are average ± SD (CV, $n = 3$). ^bData from ref 29. 1 nM mEH corresponds to 50 ng/mL mEH. All samples were diluted in 10^3 , 10^4 , and 10^5 for ELISA.

read by the microplate reader, the trends between the samples are consistently similar. The relative levels can be easily discerned by the naked eye when observing the MF membrane, indicating that the chemical immobilization of the double nanobody sandwich method on NHS@MF is feasible, highlighting the effectiveness of this analytical approach employing double nanobody sandwich ELISA.

CONCLUSIONS

In this study, double nanobody sandwich ELISAs for the detection of human microsomal epoxide hydrolase (mEH) were successfully developed, demonstrating several key advancements over traditional antibody-based assays. Our focus was on improving both the capture nanobody immobilization and the signal output of the detection antibody to explore strategies for enhancing the sensitivity of the double nanobody immunoassay. By leveraging the unique advantages of nanobodies, including their high thermal stability and specificity, we identified and optimized the MQ4–MQ30 nanobody pair, which exhibited the best performance with an LOD of 1 ng/mL.

The comparative analysis demonstrated that the use of PolyHRP effectively compensated for the lower efficiency of nonoriented nanobody immobilization, resulting in a 103-fold increase in sensitivity compared to the format using only

nanobodies labeled with HRP. Additionally, immobilizing the capture nanobody on microplates via streptavidin led to a 12-fold increase in sensitivity compared to formats that use nanobodies alone. Moreover, the use of NHS@MF membranes outperformed traditional microplates, offering a more efficient and visually intuitive platform for POCT, with a limit of detection (LOD) of 2.4 ng/mL, which is 15-fold lower than the microplate format. The advantages of each reagent immobilization method are discussed in detail elsewhere. The assays demonstrated high specificity with minimal cross-reactivity with other epoxide hydrolases and effectively mitigated matrix effects in plasma and tissue samples through the appropriate dilution strategies.

Nanobodies can be selected not only for high sensitivity but also for high specificity, often optimizing both attributes simultaneously. High specificity is highly desirable and may correlate with a high signal-to-noise ratio and enhanced sensitivity. However, it is crucial to exercise caution when applying antibody reagents across different species, as this common practice may not be reliable without proper controls. Especially in double sandwich assays, nanobodies can exhibit exceptional selectivity, making it essential to run appropriate controls with the specific protein target. For instance, data shown in Figure S7 illustrated that the dual nanobody assay developed here can distinguish between human and rat mEH

enzymes. Although it is possible to select nanobody pairs that recognize different antigenic sites on the same enzyme across species, it is important to be cautious when using an assay developed for one species to analyze proteins from another species, particularly when both capture and reporting antibodies target the same antigenic determinant. Furthermore, the thermal stability of nanobodies facilitates easy storage and transport, and the sequences provided in this study render these nanobodies as “immortal reagents” for the scientific community. These considerations highlight the potential of double nanobody sandwich ELISAs as reliable, sensitive, and stable tools for biomarker detection with promising applications in clinical diagnostics and environmental monitoring.

■ ASSOCIATED CONTENT

SI Supporting Information

The Supporting Information is available free of charge at <https://pubs.acs.org/doi/10.1021/acs.analchem.4c04505>.

Optimization experimental section for the NHS@MF-based immunoassay; thermal stability test of antibodies; optimization of concentration of streptavidin, capture antibody, and blocking conditions by SA/bioVHH/analyte/VHH-HRP format-based ELISA; optimization of blocking conditions by VHH/analyte/bioVHH/SA-PolyHRP format-based ELISA; optimization of buffer selection and concentration of capture antibody MQ4 onto NHS@MF membranes; optimization of the concentration of detection antibody MQ30-HRP onto NHS@MF membranes; optimization of image acquisition time; specificity; and accuracy and precision analysis (PDF)

■ AUTHOR INFORMATION

Corresponding Authors

Dongyang Li – College of Biosystems Engineering and Food Science, Zhejiang University, Hangzhou 310058, People's Republic of China; Email: dylee@zju.edu.cn

Bruce D. Hammock – Department of Entomology and Nematology and UCD Comprehensive Cancer Center, University of California, Davis, California 95616, United States; orcid.org/0000-0003-1408-8317; Email: bdhammock@ucdavis.edu

Authors

Qiyi He – College of Biosystems Engineering and Food Science, Zhejiang University, Hangzhou 310058, People's Republic of China; Department of Entomology and Nematology and UCD Comprehensive Cancer Center, University of California, Davis, California 95616, United States

Bofeng Pan – Biological and Agricultural Engineering, University of California, Davis, California 95616, United States; orcid.org/0000-0003-2729-8401

Mark McCoy – Department of Entomology and Nematology and UCD Comprehensive Cancer Center, University of California, Davis, California 95616, United States

Junkang Pan – College of Biosystems Engineering and Food Science, Zhejiang University, Hangzhou 310058, People's Republic of China

Zhihao Xu – College of Biosystems Engineering and Food Science, Zhejiang University, Hangzhou 310058, People's Republic of China

Christophe Morisseau – Department of Entomology and Nematology and UCD Comprehensive Cancer Center, University of California, Davis, California 95616, United States; orcid.org/0000-0002-5672-6631

Gang Sun – Biological and Agricultural Engineering, University of California, Davis, California 95616, United States; orcid.org/0000-0002-6608-9971

Complete contact information is available at: <https://pubs.acs.org/10.1021/acs.analchem.4c04505>

Notes

The authors declare no competing financial interest.

■ ACKNOWLEDGMENTS

This work was financially supported by NSFC (82273632), NKP-RD (2023YFE0119300), NIH-NIEHS (RIVER Award) R35 ES030443, and NIH-NIEHS (Superfund Award) P42 ES004699. The support from the China Scholarship Council is also acknowledged by distinguished international students' scholarship (202008440631). The authors thank Miss Brenda Le for assistance on experimental operation and statistical analysis.

■ REFERENCES

- (1) Vaclavikova, R.; Hughes, D. J.; Soucek, P. *Gene* **2015**, *571* (1), 1–8.
- (2) Lin, J.-C.; Hiasa, Y.; Farber, E. *Cancer Res.* **1977**, *37* (7), 1972–1981.
- (3) Griffin, M. J.; Noda, N.-I. *Cancer Res.* **1980**, *40* (8), 2768–2773.
- (4) Calder, P. C. *Clin. Sci. (Lond.)* **2004**, *107* (1), 1–11.
- (5) McReynolds, C.; Morisseau, C.; Wagner, K.; Hammock, B. *Adv. Exp. Med. Biol.* **2020**, *1274*, 71–99.
- (6) Fritz, P.; Mürdter, T. E.; Eichelbaum, M.; Siegle, I.; Weissert, M.; Zanger, U. M. *J. Clin. Oncol.* **2001**, *19* (1), 3–9.
- (7) Lee, W. J.; Brennan, P.; Boffetta, P.; London, S. J.; Benhamou, S.; Rannug, A.; To-Figueras, J.; Ingelman-Sundberg, M.; Shields, P.; Gaspari, L.; et al. *Biomarkers* **2002**, *7* (3), 230–241.
- (8) Zusterzeel, P. L. M.; Peters, W. H. M.; Visser, W.; Hermesen, K. J. M.; Roelofs, H. M. J.; Steegers, E. A. P. *J. Med. Genet.* **2001**, *38* (4), 234–237.
- (9) Liu, M.; Sun, A.; Shin, E. J.; Liu, X.; Kim, S. G.; Runyons, C. R.; Markesbery, W.; Kim, H. C.; Bing, G. *Eur. J. Neurosci.* **2006**, *23* (8), 2027–2034.
- (10) Hammock, B. D.; Loury, D. N.; Moody, D. E.; Ruebner, B.; Baselt, R.; Milam, K. M.; Volberding, P.; Ketterman, A.; Talcott, R. *Carcinogenesis* **1984**, *5* (11), 1467–1473.
- (11) Akatsuka, T.; Kobayashi, N.; Ishikawa, T.; Saito, T.; Shindo, M.; Yamauchi, M.; Kurokohchi, K.; Miyazawa, H.; Duan, H.; Matsunaga, T.; Komoda, T.; Morisseau, C.; Hammock, B. D. *J. Autoimmun.* **2007**, *28* (1), 7–18.
- (12) Wang, Y.; Xianyu, Y. *Small Methods* **2022**, *6* (4), No. 2101576.
- (13) Li, D.; Cui, Y.; Morisseau, C.; Gee, S. J.; Bever, C. S.; Liu, X.; Wu, J.; Hammock, B. D.; Ying, Y. *Anal. Chem.* **2017**, *89* (11), 6248–6256.
- (14) Su, Q.; Shi, W.; Huang, X.; Yin, S.; Yang, X.; Lu, X. *MedComm: Biomater. Appl.* **2023**, *2* (3), No. e54.
- (15) Zhang, J.; Sun, H.; Pei, W.; Jiang, H.; Chen, J. *J. Biomed. Res.* **2021**, *35* (4), 318–326.
- (16) Li, Z.; Wang, Y.; Vasylieva, V.; Wan, D.; Yin, Z.; Dong, J.; Hammock, B. D. *Anal. Chem.* **2020**, *92* (14), 10083–10090.
- (17) Yu, S.; Li, Z.; Li, J.; Zhao, S.; Wu, S.; Liu, H.; Bi, X.; Li, D.; Dong, J.; Duan, S.; et al. *Sensors Actuators B Chem.* **2021**, *336*, No. 129717.
- (18) Su, B.; Xu, H.; Xie, G.; Chen, Q.; Sun, Z.; Cao, H.; Liu, X. *Spectrochim. Acta A Mol. Biomol. Spectrosc.* **2021**, *262*, No. 120088.

- (19) Rossotti, M. A.; Pirez, M.; Gonzalez-Techera, A.; Cui, Y.; Bever, C. S.; Lee, K. S.; Morisseau, C.; Leizagoyen, C.; Gee, S.; Hammock, B. D.; et al. *Anal. Chem.* **2015**, *87* (23), 11907–11914.
- (20) Ren, Y.; Wei, J.; Wang, Y.; Wang, P.; Ji, Y.; Liu, B.; Wang, J.; Gonzalez-Sapienza, G.; Wang, Y. *Anal. Chim. Acta* **2022**, *1203*, No. 339705.
- (21) Li, D.; Morisseau, C.; McReynolds, C. B.; Dufлот, T.; Bellien, J.; Nagra, R. M.; Taha, A. Y.; Hammock, B. D. *Anal. Chem.* **2020**, *92* (10), 7334–7342.
- (22) Liao, X.; Zhang, Y.; Liang, Y.; Zhang, L.; Wang, P.; Wei, J.; Yin, X.; Wang, J.; Wang, H.; Wang, Y. *Anal. Chim. Acta* **2024**, *1289*, No. 342209.
- (23) Wang, Y.; Zhang, L.; Wang, P.; Liao, X.; Dai, Y.; Yu, Q.; Yu, G.; Zhang, Y.; Wei, J.; Jing, Y.; et al. *Anal. Chem.* **2023**, *95* (46), 17135–17142.
- (24) Liao, X.; Wang, J.; Guo, B.; Bai, M.; Zhang, Y.; Yu, G.; Wang, P.; Wei, J.; Wang, J.; Yan, X.; et al. *J. Agric. Food Chem.* **2024**, *72* (26), 14967–14974.
- (25) Zhang, Y.; Liao, X.; Yu, G.; Wei, J.; Wang, P.; Wang, Y.; Jing, Y.; Wang, J.; Chen, P.; Wang, J.; Wang, H.; Wang, Y. *Anal. Chem.* **2023**, *95* (36), 13698–13707.
- (26) He, Q.; McCoy, M. R.; Qi, M.; Morisseau, C.; Yang, H.; Xu, C.; Shey, R.; Goodman, M. C.; Zhao, S.; Hammock, B. D. *Int. J. Mol. Sci.* **2023**, *24* (19), 14698.
- (27) Pan, B.; He, Q.; Yu, X.; De Choch, D.; Lam, K. S.; Hammock, B. D.; Sun, G. *Talanta* **2024**, *279*, No. 126634.
- (28) Pan, B.; El-Moghazy, A. Y.; Norwood, M.; Nitin, N.; Sun, G. *ACS Sens.* **2024**, *9* (2), 912–922.
- (29) Morisseau, C.; Kodani, S. D.; Kamita, S. G.; Yang, J.; Lee, K. S.; Hammock, B. D. *Int. J. Mol. Sci.* **2021**, *22* (9), 4993.
- (30) Pan, B.; Zhao, C.; Norwood, M.; Wang, M.; Liu, G. Y.; Sun, G. *Adv. Sens. Res.* **2023**, *3* (1), No. 2300080.
- (31) Muyltermans, S. *Annu. Rev. Biochem.* **2013**, *82*, 775–797.
- (32) Joyce, A. M.; Kelly, A. L.; O'Mahony, J. A. *Int. J. Dairy Technol.* **2018**, *71* (2), 446–453.